

FIBRE REINFORCED CONCRETE: FROM FLEXURAL TESTS TO SOLID SLABS

MARCO DI PRISCO*, ALI POURZARABI[†] AND MATTEO COLOMBO[‡]

*Politecnico di Milano
Milan, Italy
e-mail: marco.diprisco@polimi.it

[†]Politecnico di Milano
Milano, Italy
e-mail: ali.pourzarabi@polimi.it

[‡]Politecnico di Milano
Milan, Italy
e-mail: matteo.colombo@polimit.it

Key words: Fibre Reinforced concrete, Slab, Reliability, Design approach

Abstract. Tensile behavior of fibre reinforced concrete is assessed based on flexural tests where specifically the post cracking strength values are of interest. However, the residual tensile strength values obtained based on such characterization test exhibit a very high scatter which is mainly due to the variation of number and orientation of fibres at the fracture plane. This rather unrepeatable behavior may cast doubt on the overall performance of a structure reinforced only with fibres and may question the validity of estimated tensile strength parameters that are used in the design of such from one specimen to another structures. While there is evidence that fibre reinforced concrete structures show a behavior that can be predicted by the average material properties, no strong proof is yet available. If so, then the low characteristic value of residual strength values may be a very conservative starting point for design of such structures To validate the reliability of design approach proposed for fibre reinforced concrete structures, twelve nominally identical fibre reinforced concrete slabs sized $2000 \times 2000 \times 150$ mm, and twelve notched specimens sized $150 \times 150 \times 600$ mm are tested, and the results are compared. Further, a yield line method is employed to predict the ultimate load bearing capacity of the slabs based on the tensile parameters obtained from the characterization tests. The results show that the average material properties can satisfactorily predict the bearing capacity of the slabs. *FraMCoS X Conference.*

1 INTRODUCTION

Fibre reinforced concrete (FRC) has very attractive features both in terms of mechanical and durability properties [1, 2]. Considerable post-cracking residual strength in a FRC material can significantly increase the load bearing capacity of structural elements and limit the opening of cracks. Complete or partial exclu-

sion of conventional rebars can remarkably reduce the labor cost and allow for more architecturally pleasant forms to be cast. Although has a higher cost of production, FRC can yet bring savings in the total costs by reducing the volume of material and by cutting construction costs [3]. To better place this material in a cost-driven market, it is of paramount importance to

exploit its capacity to its full extent.

The tensile behavior of a FRC material is commonly characterized through a flexural test on standard beam specimens with or without a notch. In either case, the results obtained for residual tensile strength parameters from such testing methods exhibit a high scatter. Propagation of a single crack at the position of the notch in a three point bending test, or at very few locations, if ever, in a four-point bending test, makes the response of these testing methods very dependent on the number and orientation of fibres at a single cross section along the beam specimen, which can considerably vary from one specimen to the other depending on the casting method. This is unlike the behavior of FRC structural elements that show a highly repeatable structural response. Consequently, a low characteristic value for material tensile properties sets a starting point for design of a FRC structure, which leads to overly safe structures. Filling the unnecessarily large gap between the computed design resistance of a structural element with what may be obtained in a real-life case is a reservoir of strength that if left unnoticed, may undermine the sustainability of FRC as a structural material.

In this work, to examine the extent to which a Steel Fibre Reinforced Concrete (SFRC) structure outperforms the predictions coming from a design perspective, we have tested twelve notched prismatic beams following the EN 14651 [4] methodology in a three-point bending setup, and twelve nominally identical slabs that were reinforced only with steel fibres while being supported on four corners and loaded in the center.

2 EXPERIMENTAL PROGRAM

2.1 Materials and specimens

A self-consolidating SFRC material is used to cast all the specimens whose mix design is given in Table 1. The mix design contains 35 kg/m^3 of double hooked steel fibres with a length of 60 mm and a diameter of 0.9 mm. The fibres have a tensile strength of 1500 MPa and a Young's modulus of 210 GPa.

Table 1: Mix design of the SFRC material

Cement (Cem IV 42.5) [kg/m^3]	380
Sand 0/4 [kg/m^3]	425
Sand 0/8 [kg/m^3]	850
Gravel [kg/m^3]	425
Carbonate filler [kg/m^3]	100
w/b	0.36
Fibre [kg/m^3]	35
Superplasticizer (% of cement weight)	1.2

Twelve $150 \times 150 \times 600$ mm prismatic beams and twelve $2000 \times 2000 \times 150$ mm slabs were cast in a job-site from the same concrete batch that was delivered by a truck mixer. The slabs were cast from the center of the molds and the flowability of the concrete obviated any need for vibration. After casting, all the specimens were covered with a moist burlap for a couple of days, and afterwards they were transferred to the laboratory where they were kept in atmospheric condition until the age of testing. At each testing age we tested one notched beam and a companion slab. Further, six cubes with a 150 mm side were cast together with the slabs and prismatic beams for the assessment of the compressive strength. Three of the cubes were tested on the first testing age at 59 days, and three of the cubes were tested on the last day of testing, at 134 days. The average compressive strength obtained was respectively 47.4 and 59.8 MPa with a coefficient of variation of 3% for both testing ages.

2.2 Three-point bending test

The prismatic beams were notched in the mid-length to a depth of 25 mm and were tested in a three-point bending scheme according to EN 14651 with a span of 500 mm. During the test the Crack Mouth Opening Displacement (CMOD) was measured with a clip gauge at the notch. The results of the test are represented in terms of nominal stress-CMOD. Specifically, according to the EN 14651 and the fib Model Code 2010 [5], the values of nominal residual stress at a CMOD of 0.5, 1.5, 2.5, and 3.5 mm are reported as f_{R1} , f_{R2} , f_{R3} and f_{R4} .

2.3 Slab test

The twelve slabs were tested under a central concentrated load and they were supported at the four corners on square steel plates of $200 \times 200 \times 25$ mm welded on top of a steel column made of two UNP200 profiles. An electro-mechanical jack with a capacity of 1000 kN was used and a constant displacement rate of $20 \mu\text{m}/\text{sec}$ was imposed to the loading head. A piece of neoprene sheet was placed between the slab and supports and beneath the loading point to prevent erratic local effects. The slabs were connected to the supports by means of an anchorage device to create a bilateral restraint. However, measurements on the rotation of the slab corners showed that for the most part of the test, the anchorage device is not in tension, and in fact the slabs are allowed to rotate at the supports. The details on the support dimensions and placement can be found in [6]. A schematic representation of the slab setup is shown in Figure 1.

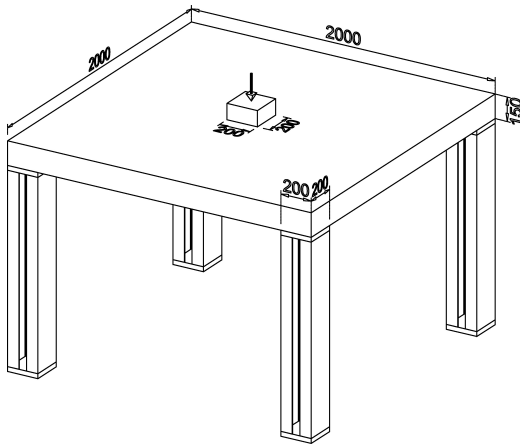


Figure 1: Schematic representation of the dimensions of the slab.

For each slab, the deflection is measured from the bottom of the slab at the center. Furthermore, ten measurements are carried out to detect the propagation of cracks on the slabs by means of LVDTs (Linear Variable Differential Transducer). The position, gauge length, and the label of these instruments are shown in Figure 2. Four instruments are positioned on the top surface of the slabs at the location of

the supports to capture possible negative cracks, which are shown by COD_t and two letters showing its position in the plane of the slab. Six instruments record the propagation of cracks at the bottom of the specimens. The four instruments in the center of the slab are designated by COD_b and the two longer instruments are marked with CODL_b . These are accompanied by one letter showing the direction of the instruments.

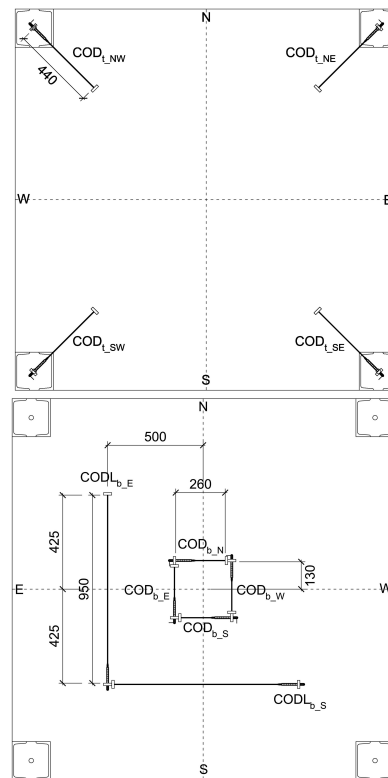


Figure 2: Position, label, and gauge length of instruments on (top) top face; and (bottom) bottom face of slabs.

3 Results and discussion

3.1 Notched beams

Figure 3 shows the results of the tests carried out on the notched beams in terms of nominal stress-CMOD. On the figure, the gray area shows the scatter of the results, the black solid line is the average of the curves, and the solid grey line is the characteristic curve corresponding to a 5% percentile considering a lognormal distribution for the residual strength values.

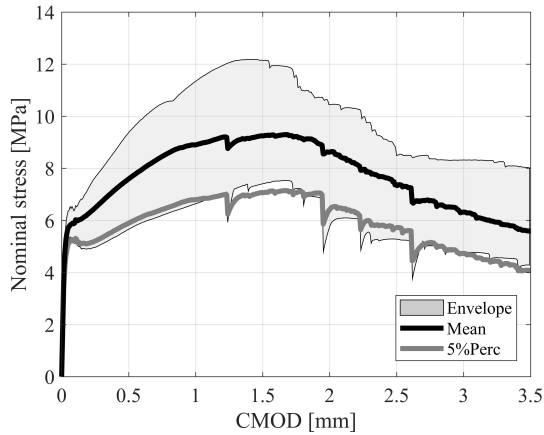


Figure 3: Stress-CMOD result of twelve tested notched beam specimens.

The stress-CMOD results show that after cracking, the SFRC material exhibits a hardening behavior up to a CMOD of approximately 1.5 mm, and then comes the softening phase. The residual strength values with statistical parameters obtained for these values are reported in Table 2. According to the classification methodology suggested in the MC 2010 the SFRC material is categorized as a "5c". In view of the focus of the present work, the dispersion of these results is of specific interest where a coefficients of variation in the range of 15% to 19% is obtained.

Table 2: Results obtained from the notched beam tests with statistical parameters

	Average [MPa]	5% percentile [MPa]	V*[%]
$f_{ct,fl}$	5.7	4.9	7
f_{R1}	7.6	5.6	15
f_{R2}	9.3	6.7	17
f_{R3}	7.7	5.4	16
f_{R4}	5.8	4.0	19

*coefficient of variation

3.2 SFRC slab behaviour

Figure 4 shows the load-deflection result of each of the twelve tested slabs. The tests were stopped, and the specimens were unloaded, upon demonstration of a softening behavior. Other than two of the slabs that show an er-

atic different initial stiffness, the other elements show an almost equal initial slope in the load-deflection response. After this initial linear phase, the slabs display a hardening behavior before going through a softening response. The average of the maximum load sustained by the slabs is 132.2 kN with a coefficient of variation of 5.2%. The characteristic value of the maximum load considering a lognormal distribution is 122.9 kN. The dispersion of the structural maximum load is considerably different from that of the residual tensile strength values that were obtained in case of the notched beam tests. This stark difference highlights the in-born distinction between the structural test, and a characterization test carried out on the same SFRC material.

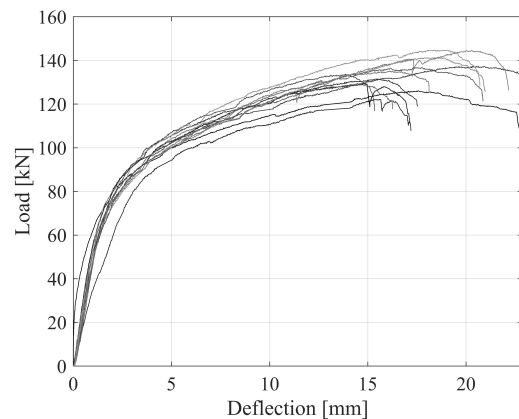


Figure 4: Load-deflection response of the twelve slabs.

As compared to the maximum load, the deformation capacity of the slabs shows a higher variation. The deflection corresponding to the maximum load has an average of 16.2 mm with a coefficient of variation of 13%. Overall, slabs reinforced only with fibres may show limited ductility as opposed to R/C slabs, which needs attention when dealing with slabs without conventional reinforcement and where ultimate limit state is of concern. This was shown earlier in [6] where the behavior of SFRC slabs and R/C ones were compared. The results presented here show that for SFRC slabs, determination of the maximum deflection may also be subjected to a rather high uncertainty.

In Figure 5 the crack pattern at the bottom of one of the SFRC slabs is presented as an example. In all slabs two perpendicular bands of cracks are formed stretching from the middle of one side to the opposite side. In the middle of the slabs and beneath the loading point the cracks show a more irregular pattern, however, away from this zone cracks show a parallel configuration. The average spacing of the cracks at the edge of the slabs varies from around 60% of the slab depth to 150 mm which is the slab depth. No cracks appeared on the top face of the slabs and therefore the results recorded by COD_t instruments are not discussed and reported here. It is also pointed out that the detection of the cracks has been done visually and cracks has been marked at different loading levels.

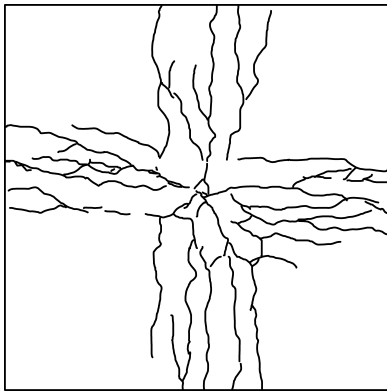


Figure 5: The bottom-crack pattern of one of the slabs.

The measurements carried out on the propagation of cracks at the bottom of the slabs with the COD_b and $CODL_b$ instruments are shown in Figure 6. Taking into account the recordings made by each single instrument, it is noted that at a certain load level in each slab, the deformation is concentrated in those instruments that capture the localized cracks, while the other measurements show constant or slightly decreasing values. In Figure 6, only the measurements that capture the localized crack are reported and they are averaged for each specimen for the instruments of the same group. In Figure 6(bottom) ten curves are presented as the results measured for two of the slabs were lost due to

technical problems.

In general, the curves obtained for the crack opening measurements in the slabs are similar to those of the deflection response. Table 3 reports the average load and the coefficient of variation of load level at crack openings of 0.5, 1.5 and 2.5 mm measured by COD_b and $CODL_b$ instruments. The values of coefficient of variation fall below 5% which indicates that not only the SFRC slabs show a very repeatable structural response in terms of load-deflection, but also the cracking behavior of these elements is very similar. While not a sound comparison, the distinction between the behavior of the notched beams and the slabs may also be underlined by looking at the coefficient of variation at corresponding crack openings, where in the slabs, these values are less than three times of those of the notched beams for the same value of crack opening.

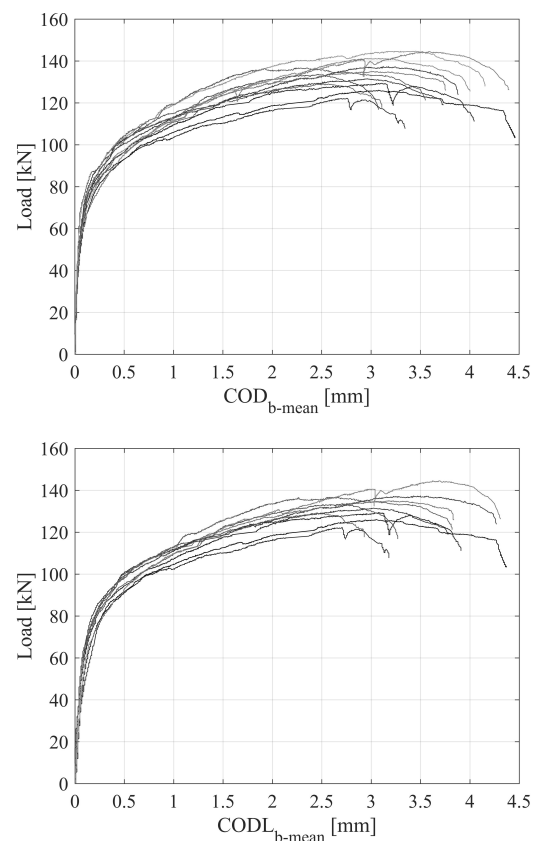


Figure 6: Crack opening measurement on the slabs with (top) COD_b instruments in the center; and (bottom) two $CODL_b$ instruments. The results are averaged for those recordings that capture the localized crack.

Table 3: Average load and coefficient of variation of load for the slabs at a COD_b and $CODL_b$ of 0.5, 1.5, and 2.5 mm

	COD (mm)	Load _{ave} (kN)	V _{Load} (%)
COD _b	0.5	98.9	4.1
	1.5	121.7	4.8
	2.5	131.4	4.7
CODL _b	0.5	96.2	3.8
	1.5	118.8	4.5
	2.5	129.4	5

4 ULTIMATE LOAD PREDICTION

A yield line approach is adopted to compare the experimental average and characteristic resistant load of the slabs with those that would be obtained following a limit state analysis starting from average and characteristic values of material properties that were determined from the characterization tests. Further, the design resistant load that would be obtained from such an approach is also compared with the experimental values. To do so, the yield line pattern shown in Figure 7 is considered which also coincides with the experimental failure mechanism.

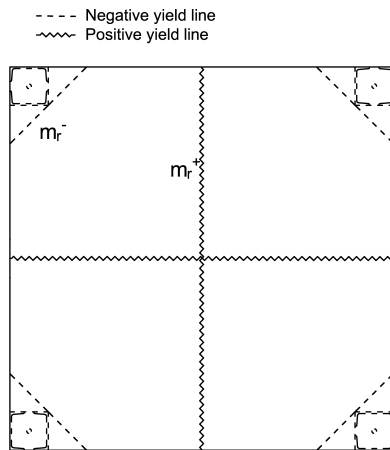


Figure 7: The yield line pattern considered for prediction of the resistant load.

For the tensile behavior of the SFRC material the provisions of MC 2010 is followed. A plane section approach is assumed for the computation of the positive and negative resisting bending moments and the chosen characteristic length equals the depth of the slab, 150 mm.

Figure 8 shows the tensile constitutive behavior of the SFRC for the mean, characteristic and design value of material properties. The design value of material properties is obtained by introducing a partial safety factor of 1.5.

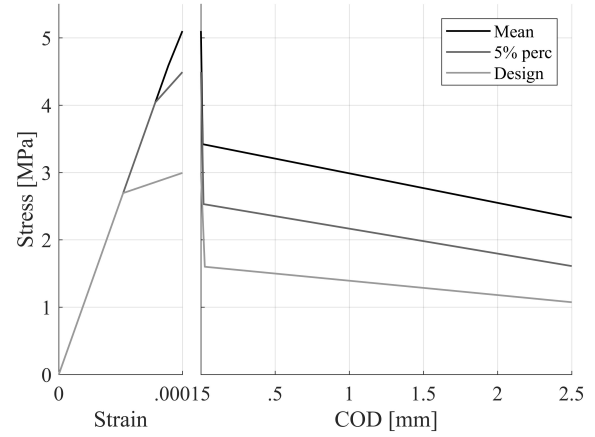


Figure 8: The tensile constitutive law of the SFRC material based on average, characteristic, and design value of strength values.

The development of the formulations to derive the ultimate resistant load according to the selected yield line pattern results in an almost 70% contribution from the positive bending moment and 30% from the negative bending moment ($P_u = 5m^+ + 2m^-$). However, experimental evidence shows that no negative cracks appeared during the tests on the SFRC slabs which owes mainly to the specific support condition adopted in the study which allows the rotation of the slab corner. The ductility of the slabs could not accommodate the formation of the negative cracks at the support position before the unfolding of the softening phase. Hence, introduction of the m^- in the formulation may unrealistically overestimate the load bearing capacity of the slabs. Therefore, the ultimate load of the slabs is computed once with the assumption of the presence of the negative cracks and once without their contribution. The computation is carried out with the mean, 5% percentile, and design tensile constitutive relations which are shown in Figure 9 with horizontal lines marked with m , k , and d letters. Furthermore, Figure 9 shows the envelope of the ex-

perimental results with the mean and characteristic value of the experimental load-deflection results.

According to Figure 9, it is clearly observed that adoption of a failure mechanism that comprises the negative cracks which does not match the experimental crack pattern, will substantially overestimate the resistant load of the slabs. On the contrary, excluding the negative cracks from the computations and implementing the mean tensile constitutive relation, gives a very close prediction for the average resistant load. The predicted ultimate load is 128 kN as opposed to the 132.2 kN obtained experimentally. This evidence draws attention to the importance of adopting a proper failure mechanism when performing a yield line approach. Measures should be taken to assure sufficient structural ductility so that the predicted failure mechanism, conforms with the real-life crack patterns [6]. Nevertheless, in a monolithic structure the support rigidity may suffice to trigger the creation of negative cracks.

In case of the yield line pattern that corresponds with experimental evidence, it is remarkable to notice the difference between the experimental characteristic maximum load (the maximum on the solid grey line in Figure 9), and the one obtained from the yield line method by means of the characteristic tensile properties. Although the average material properties nicely catches the average structural response of the slabs, the high scatter of the residual tensile strength parameters leads to a very conservative prediction for the characteristic maximum load, and since a structural design procedure is based on characteristic properties of material parameters, the excessive safety margin compromises the efficiency of structural applications of FRC materials. In an economical structural design, the design value of resistance equals the design value of load effects, although in practice the design value of resistance is larger which provides additional safety margin [7]. Therefore, ideally, we aim to predict the characteristic behavior of the structure with the characteristic material properties. Here, the predicted

characteristic resistant load is 91 kN versus the 122.9 kN of the experimental results, which gives a ratio of $P_{u-Exp}/P_{u-Predicted}=1.35$. Hence, the computed design resistant load can be increased with a factor of 1.35 without penalizing the required reliability level. This is in accordance with the idea of the redistribution factor, κ_{Rd} , introduced in the MC 2010, which allows the magnification of the computed design resistant load computed by using characteristic strengths for FRC structures that are capable of redistributing stresses. This topic has also been discussed elsewhere [8].

Table 4 reports the predicted values for both yield line patterns and for the three state of material properties and the ratios with respect to the experimental values. Assuming that the design resistance could be increased by a factor of 1.35, the final design resistant load would be $59 \times 1.35 = 79.6$ kN, which leads to a safety factor of $\gamma_s = 127.9/79.6 = 1.6$.

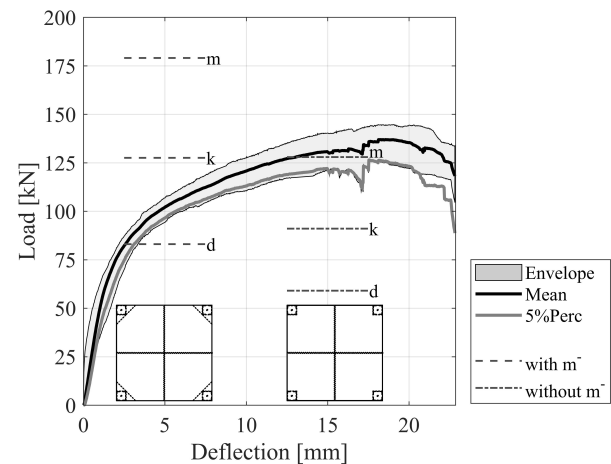


Figure 9: Ultimate load prediction of the SFRC slabs by means of a yield line approach with mean, characteristic and design value of tensile constitutive relations for the cases with and without the negative cracks.

5 CONCLUSIONS

We have discussed and compared the difference in the scatter of results of twelve notched beams tested in a three-point bending test and the structural response of twelve slabs made of a SFRC material and have highlighted the consequences of such distinction. The deflection re-

Table 4: Experimental mean and characteristic values of resistant load and the predicted values following a yield line approach

Material properties	Experimental load	With m^-		Without m^-	
		Pu_{Exp} (kN)	$Pu_{Exp}/Pu_{Predicted}$	Pu_{Exp} (kN)	$Pu_{Exp}/Pu_{Predicted}$
Mean	132.2	179	0.74	127.9	1.03
5% perc	122.9	127.5	0.96	91	1.35
Design	-	83	-	59	-

sponse and the cracking behavior of the twelve SFRC slabs were closely repeated with a coefficient of variation lower than 5%. This was despite of the fact that the same SFRC material showed a coefficient of variation between 15% to 19% in the post-peak tensile strength in the characterization tests. Unlike the load carrying behavior, the ductility of the SFRC slabs was subjected to more variation with a coefficient of variation of 13% for the deflection corresponding to the maximum load with the minimum and maximum values being 13.9 mm and 20.1 mm.

We then predicted the design resistant load of the SFRC slabs with the mean, 5% percentile, and the design value of material properties through a yield line approach. We observed that adoption of a yield line pattern that does not correspond with the experimental crack, can lead to unsafe prediction of the maximum load. Further, we showed that the mean material properties can well predict the maximum load sustained by the slabs, while the very conservative values of characteristic tensile strength parameters, greatly underestimates the 5% percentile of the maximum load in the slabs with a ratio of 1.35. Finally, the design resistant load obtained from the yield line procedure was magnified by the 1.35 coefficient which led to a reasonable safety factor of 1.6 for the slab.

References

- [1] di Prisco, M., Felicetti, R., and Plizzari, G.A. *PRO 39: 6th International RILEM Symposium on Fibre-Reinforced Concretes (FRC) - BEFIB 2004 (Volume 1)*. RILEM, 2004.
- [2] Berrocal, C.G., Löfgren, I., and Lundgren, K. The effect of fibres on steel bar corrosion and flexural behaviour of corroded rc beams. *Engineering Structures*, 163:409–425, 2018.
- [3] Blanco, A., de la Fuente, A., and Aguado A. Sustainability analysis of steel fibre reinforced concrete flat slabs. In *II International conference on concrete sustainability ICCS16*, 2016.
- [4] EN 14651: Test method for metallic fibered concrete-Measuring the flexural tensile strength (limit of proportionality (LOP), residual). *Brussels: European Committee for Standardization*, 2005.
- [5] Fédération internationale du béton. *Model code 2010: final draft*. International Federation for Structural Concrete (fib), Lausanne, Switzerland, 2013.
- [6] di Prisco, M., Colombo, M., and Pourzarabi A. Biaxial bending of sfrc slabs: Is conventional reinforcement necessary? *Materials and Structures*, 52(1):1, 2019.
- [7] Gulvanessian, H. and Holicky M. Eurocodes: using reliability analysis to combine action effects. *Proceedings of the Institution of Civil Engineers-Structures and Buildings*, 158(4):243–252, 2005.
- [8] di Prisco, M., Martinelli, P., and Parmentier P. On the reliability of the design approach for frc structures according to fib model code 2010: the case of elevated slabs. *Structural Concrete*, 17(4):588–602, 2016.